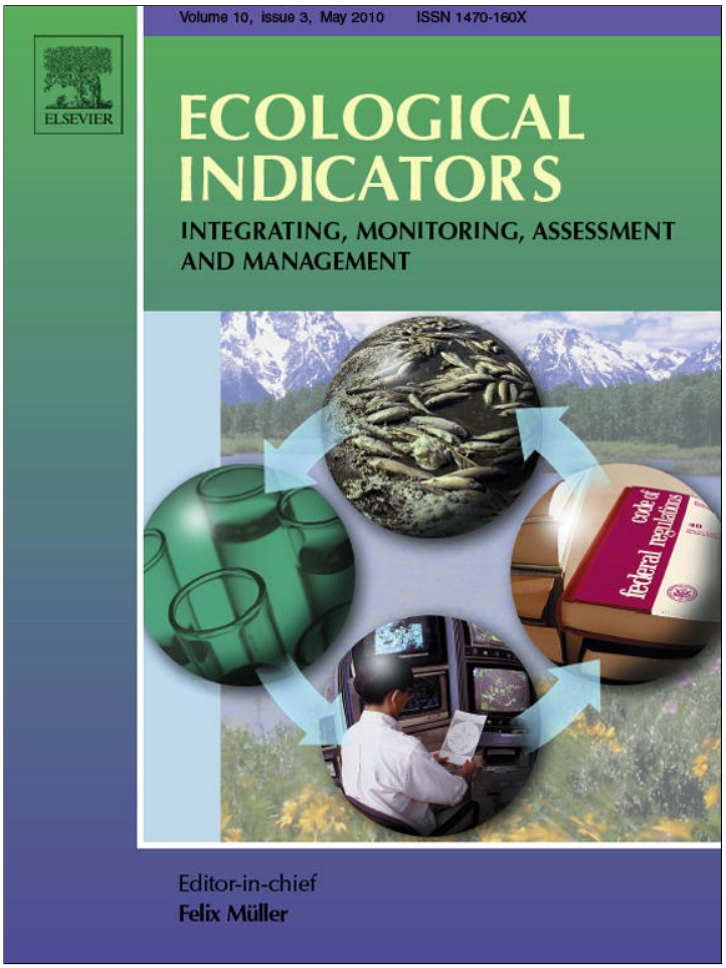

Ecological Indicators 10 (2010) 657–667

Contents lists available at ScienceDirect

Ecological Indicators

journal homepage: www.elsevier.com/locate/ecolind

Calibrating vascular plant abundance for detecting future climate changes in Oregon and Washington, USA

Timothy J. Brady [a,*], Vicente J. Monleon [b], Andrew N. Gray [b]

[a] Department of Biology, Harney Science Center 342, University of San Francisco, 2130 Fulton Street, San Francisco, CA 94117-1080, USA
[b] USDA Forest Service, Pacific Northwest Research Station, 3200 SW Jefferson Way, Corvallis, OR 97331, USA

ARTICLE INFO

Article history:
Received 4 April 2009
Received in revised form 8 October 2009
Accepted 5 November 2009

Keywords:
Vascular plant species
Climate indicators
Transfer functions
Canonical correspondence analysis
Weighted averaging-partial least squares regression

ABSTRACT

We propose using future vascular plant abundances as indicators of future climate in a way analogous to the reconstruction of past environments by many palaeoecologists. To begin monitoring future short-term climate changes in the forests of Oregon and Washington, USA, we developed a set of transfer functions for a present-day calibration set consisting of climate parameters estimated, and species abundances measured, at 107 USDA Forest Service FIA (Forest Inventory and Analysis) Phase 3 plots. For each plot, we derived climate estimates from the Daymet model database, and we computed species abundance as quadrat frequency and subplot frequency. We submitted three climate variables (mean January temperature, MJAT; mean July temperature, MJUT; and mean annual precipitation transformed to natural logarithms, MANPt) to canonical correspondence analysis (CCA), and verified their importances in structuring the species frequency data. Weighted averaging-partial least squares regression (WA-PLS) provided the means for calculating six transfer functions. In all cases, based on performance statistics generated by leave-one-out cross-validation, we identified two-component WA-PLS models as the most desirable. The predictive abilities of our transfer functions are comparable to, or better than, those reported in the literature, probably due both data quality and statistical considerations. However, model overfitting as a result of spatial autocorrelation remains a possibility. The large errors associated with our MJAT transfer functions connote that even the highest amount of change in mean January temperature predicted for Oregon and Washington for 2010–2039 would be indistinguishable from current conditions. The higher predictions indicate that our MJAT transfer functions may be able to track climate changes by the 2040s. Our MJUT transfer functions can detect change in mean July temperature under the highest projection for 2010–2039. Our MANPt transfer functions will be of limited use until the 2070s, given the predictions of only slight changes in mean annual precipitation during the early part of the twenty-first century. Our MJAT and MANPt transfer functions may prove useful at the present time to verify relative climatic stability. Because the predicted climate values sometimes deviate substantially from the observed values for individual plots, our transfer functions are appropriate for monitoring climatic trends over the entire Pacific Northwest or large regions within it, not for assessing climate change at individual plots.

1. Introduction

Climate significantly affects the growth rates and equilibrium abundances of populations of vascular plants, and therefore, it influences their evolutionary histories through natural selection (Enright, 1976; Woodward, 1987, 1992; Woodward and Williams, 1987). In effect, the genomes of vascular plant species contain information about past and present climates. If properly calibrated, an assemblage of vascular plants should provide a quantitative signal of site-specific climatic conditions. The use of vascular plant species as indicators potentially offers very high-resolution data on local climate where instrumentation is unavailable (e.g., in remote mountainous locations). Given the recent and expected future rapid climate change (e.g., IPCC, 2007), decision makers demand high quality quantitative descriptions of local climate at successive time intervals (Hartmann et al., 2002; Miles et al., 2006). Vascular plant indicators may help meet this need, but they may also provide information regarding the biological impact of changing climate.

Outside of palaeoecology, few researchers have used vascular plants as indicators for obtaining quantitative estimates of local climate variables: Karlsen and Elvebakk (2003) mapped local temperature variations in East Greenland using an "Index of Thermophily", a combination of a plant species' summer temperature needs (determined by geographical distribution), its local

* Corresponding author. Tel.: +1 415 422 5741; fax: +1 415 422 6363.
E-mail address: brady@usfca.edu (T.J. Brady).

1470-160X/$ – see front matter © 2009 Elsevier Ltd. All rights reserved.
doi:10.1016/j.ecolind.2009.11.004

abundance, local habitat diversity, and the local proportion of unproductive land. More recently, Garbolino et al. (2007) determined the climate affinities of nearly 2000 vascular plant species in France based on correlations between the geographical distributions of relevés and meteorological stations. For each of six climate variables, they calculated an affinity as a function of a species' maximum frequency and the dispersion of its frequencies around the maximum. Using vascular plants as indicators, the authors produced detailed climate maps of France.

Since the 1970s, many palaeoecologists have employed vascular plants as indicators to derive quantitative climatic information about local or regional late-Quaternary environments (recent examples include Finsinger et al., 2007; Li et al., 2007; Neumann et al., 2007; Wilmshurst et al., 2007; St. Jacques et al., 2008). These researchers have sought to develop transfer functions, multivariate equations that permit the estimation of ancient climate parameters from data on fossils (Birks, 1995, and references therein). Calibration sets, which include spatially correlated present-day climatic conditions and pollen grain/pteridophyte spore/phytolith counts, specify the transfer functions. Formally, **C** (a matrix of n standardized observations, one at each of n locations on q climate variables), **X** (the corresponding matrix of standardized observations on p biological variables at each of the same n locations), β (a matrix of transfer functions, one for each of the q climate variables, with each comprised of p elements), and δ (a matrix of random noise, with n parts for each of the q climate variables) are related through a linear model:

$$\mathbf{C} = \mathbf{X}\boldsymbol{\beta} + \boldsymbol{\delta} \quad (1)$$

β acts as a set of transfer functions, because observations on the p biological variables render estimates of the q climate variables.

The use of vascular plants to monitor climate carries the assumption that their populations are always in dynamic equilibrium with climate (Davis and Botkin, 1985; Webb, 1986; Prentice et al., 1993): the list of species in a community and their properties (e.g., abundances) match those allowable under the prevailing climatic regime. If the biological response lags significantly behind the pace of climate change, then this assumption is unjustified. Davis and Botkin (1985) showed, through simulation studies, that short-term (i.e., decadal) climate changes may have little immediate effect on the adult survival of long-lived tree species. Even annuals and short-lived perennials may be little affected by climate change as long as the buffering capacity of the canopy persists (Smith, 1965; Davis and Botkin, 1985). Regular disturbance may be necessary to guarantee that short-term climate change will bring about a measurable species response.

Palaeoecologists use the past remains of vascular plants as indicators of past climate. Transfer functions provide the means of translating past biology into quantitative estimates of past climate. We propose that foresters and environmental scientists adopt a parallel approach: use future data on vascular plants as indicators of future climate. Transfer functions will furnish the link between future biology and future climate. In the present study, we took the first step in establishing a program for monitoring future short-term climate changes in the forests of Oregon and Washington, USA, based on vascular plant abundances: We developed a set of transfer functions for a calibration set consisting of a few estimated climate parameters and species abundances measured at 107 locations.

2. Materials and methods

2.1. Data on vascular plant abundance

We derived vascular plant abundances from inventory data for USDA Forest Service FIA (Forest Inventory and Analysis) Phase 3 plots, which represent a systematic subset of the inventory plot grid that spans the forestlands of the USA. The density of Phase 3 plots is about one per 390 km^2. Each plot consists of a cluster of four 168 m^2 non-overlapping subplots, arranged within a 1 ha circle. Each subplot contains three 1 m^2 quadrats. Field crews recorded the presence and cover of each species with heights of up to 1.8 m on each quadrat. They subsequently searched the subplots for up to 45 min to find additional vascular plant species of any height that occur outside the quadrats. Vegetation sampling of Phase 3 plots occurs during June, July, or August, and, if fully implemented, remeasurement would take place on the standard inventory cycle (10 years in the western USA). Stapanian et al. (1997) and Schulz et al. (2009) provide detailed information about the design and sampling of FIA Phase 3 plots.

Cover values reflect the vagaries of phenology, weather conditions, field crew biases, and actual abundance (Gray and Azuma, 2005; Smith et al., 1986; Schulz et al., 2009). As an alternative, we computed two frequency measures for each species present on a given plot. For species i, Fq_i is quadrat frequency and Fs_i is subplot frequency:

$$Fq_i = \frac{(\text{number of quadrats on which species } i \text{ occurs})}{12} \quad (2)$$

$$Fs_i = \frac{(\text{number of subplots on which species } i \text{ occurs})}{4} \quad (3)$$

Both Fq_i and Fs_i vary from 0 to 1. Quadrat frequency and subplot frequency provide rough yardsticks of abundance, not just distribution, of a species within an FIA Phase 3 plot. Adult survival, fecundity, within-plot dispersal, and the survival of recruits dictate the frequency of a vascular plant species. While they are not synonymous with population density, Fq_i and Fs_i convey information about the proportion of a plot occupied by a species. A plant species with a large population, as measured by cover value, should occupy a larger proportion of a plot than a species represented by a small population (Andrewartha and Birch, 1954; Krebs, 1985).

Like all frequency measures, Fq_i and Fs_i depend on plot size. Thus, we excluded from consideration any plot comprised of less than 100% accessible forest, as it would have sampled fewer than 12 quadrats and fewer than four subplots.

For construction of the calibration set, we obtained data from 107 fully forested FIA Phase 3 plots sampled in 2001, 2004, and 2005 distributed across Oregon and Washington (Fig. 1). We calculated quadrat frequencies for 538, and subplot frequencies for 698, vascular plant species on these plots. In view of recent findings (Lischke et al., 2002; Miller et al., 2008; Payette, 2007; Svenning et al., 2008; Valsecchi et al., 2008), we expect that any lag in response (a delay in adjustment of species frequency on a plot) to climate change will depend upon the complex interplay of many factors such as species autecology (including vagility), forest stand structure (resulting from intra- and interspecific interactions as well as disturbance regime), soil development, and geographical impediments to migration (e.g., rugged terrain and habitat fragmentation). The immediacy of response may vary among species on the same plot, and even among plots for the same species. We cannot possibly predict the speeds of species responses, especially since most species analyzed here are poorly known ecologically. Therefore, we included a broad array of plant functional types in this study (e.g., annuals, short-lived perennials, ruderals, and long-lived perennials) to increase the likelihood of obtaining rapid and significant changes in frequency by at least some species on each plot following short-term climate change. Unlike conventional palaeoecological practice, we did not exclude rare species from the calibration set. While this maneuver

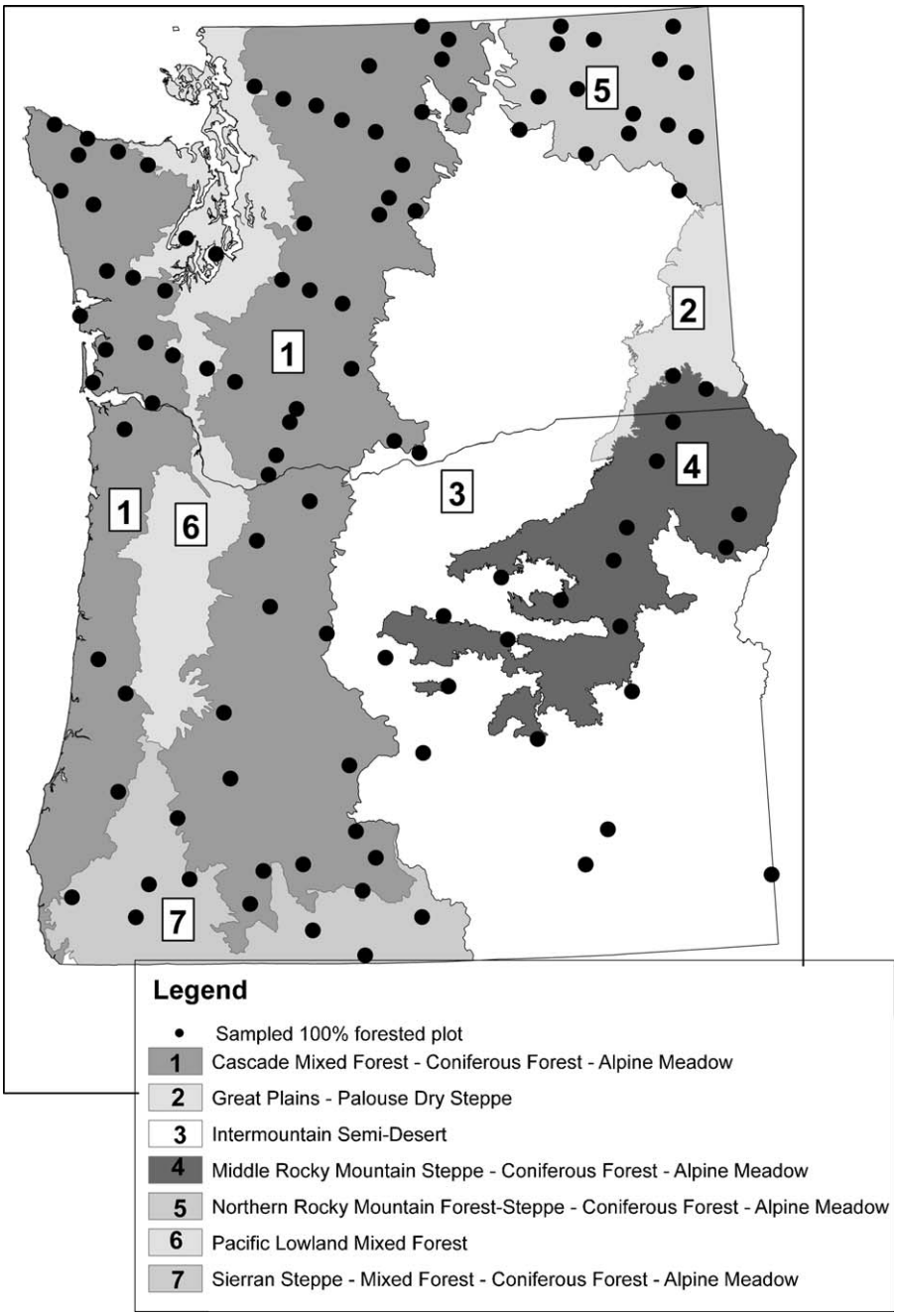

Fig. 1. Map of Oregon and Washington showing the locations of 107 FIA Phase 3 plots included in the calibration set. Vegetation classification follows Cleland et al. (2007).

engenders the risk of producing poorly performing transfer functions, it may increase the sensitivity of our analysis.

2.2. Climate data

To obtain valid approximations of local climatic conditions in Oregon and Washington after 2005, the calibration set must sample the full range of future climates in these two states (Sachs et al., 1977; Howe and Webb, 1983). Given the pronounced climatic diversity of Oregon and Washington (climate varies from maritime to continental, with strong orographic and rainshadow effects caused by numerous tall [>3000 m] mountain ranges; Franklin and Dyrness, 1988), we expect that most future shifts in climate will result in conditions at one location that match those found today somewhere in the study area. Of course, this assumes that climate change will not reduce the fully forested condition of a plot.

We sought to use vascular plant species as indicators of four general climate variables: (1) mean annual temperature (°C; here symbolized MANT), (2) mean January temperature (°C; here symbolized MJAT), (3) mean July temperature (°C; here symbolized MJUT), and (4) mean annual precipitation (mm; here symbolized MANP). We obtained a plot-specific 18-year (1980–1997) average for each of these variables by intersecting plot locations with data from Daymet (Thornton et al., 1997; database at http://www.daymet.org/), a high-resolution (1 km grid) model developed for the conterminous USA from elevation data, topographic indices, daily observations from ground-based meteorological stations, and statistical algorithms.

Table 1
Descriptive statistics associated with the frequency distributions of climate variables over 107 FIA Phase 3 plots.

	MANT (°C)	MANP (mm)	MJAT (°C)	MJUT (°C)	MANPt
Minimum	−1.15	271.50	−10.81	8.07	5.60
Maximum	11.97	4979.00	6.40	21.82	8.51
Mean	6.72	1386.00	−1.29	15.69	7.03
Standard deviation	2.66	873.40	4.09	2.26	0.67
Median	7.02	1053.00	−1.90	15.46	6.96

MANT = mean annual temperature, MANP = mean annual precipitation, MJAT = mean January temperature, MJUT = mean July temperature, MANPt = mean annual precipitation transformed to natural logarithms.

The temperature variables (MANT, MJAT, and MJUT) were roughly normally distributed to slightly negatively skewed. However, MANP was severely positively skewed, due to very high precipitation values near the Washington coast. We transformed the mean annual precipitation data to natural logarithms (MANPt symbolizes the transformed variable) to produce an approximately normal distribution. While the statistical techniques used in this study do not require a normal frequency distribution over plots for a climate variable, a reduction in skewness improves transfer function performance. Table 1 gives descriptive statistics for the frequency distributions of MANT, MANP, MJAT, MJUT, and MANPt.

2.3. Climate variable selection and evaluation

In the spirit of parsimony and to comply with the requirements of the statistical techniques used here, we sought to minimize redundancy (multicollinearity) among the climate variables included in our analyses. We calculated variance inflation factors (VIFs; Marquardt, 1970) for all climate variables with JMP 4.0.2 (SAS Institute Inc., 2000). The VIF for MANT was >10, which according to Belsley et al. (1980), indicates a high degree of multicollinearity. Therefore, we eliminated MANT from further analysis. This reduced the VIFs for the remaining variables to <4.

The methods employed here assume that the frequencies of vascular plants are significantly correlated with climate variables, but only weakly linked to non-climatic factors (Birks, 1998, and references therein). We used canonical correspondence analysis (CCA; Ter Braak, 1986, 1987), to evaluate the relationship between the biological and climate variables in the calibration set, and to determine which variables we should include in the transfer functions. CCA performs best when species abundance (here, quadrat frequency or subplot frequency) is a symmetrical unimodal function of each environmental variable (here, each of the climate parameters).

Species responses typically appear linear when gradients are short, but they tend to assume non-linear forms when gradients are long (Leps and Smilauer, 2003; Økland, 1986; Ter Braak and Prentice, 1988; Ter Braak, 1995). We used detrended correspondence analysis (DCA; Hill and Gauch, 1980), to estimate the gradient lengths within the calibration set with PC-ORD 5.0 (McCune and Mefford, 2005). The program downweighted rare species, divided each axis into 30 segments, and evaluated the ability of DCA to recover compositional gradients by calculating, for each axis, a coefficient of determination (r^2) between Euclidean distance in the ordination space and relative Euclidean distance in the original species frequency space (McCune and Grace (2002) recommend the use of relative Euclidean as a distance measure for the original space under DCA). The calculated gradient lengths for the quadrat and subplot frequencies were over seven standard deviation units for the first two DCA axes, and the two axes explained 0.40 and 0.55 of the variance for quadrats and subplots, respectively. These figures are large for species-rich data with numerous zero abundance values. The large gradient lengths, which are not unexpected given the marked ecological diversity of the Pacific Northwest (Franklin and Dyrness, 1988), represent the longest compositional gradients reported in the literature for vascular plant transfer function studies. They strongly suggest that species responses to MJAT, MJUT, and MANPt are non-linear.

We used the fitting procedure of Huisman et al. (1993) to decide whether the relationships between species abundance and climate are best approximated by a symmetrical unimodal model or by one of three other non-linear functions. The alternatives (so-called HOF models) are elements of an hierarchical set: a skewed unimodal response (model V), a symmetrical unimodal response (model IV), a monotonic increase or decrease with plateau (model III), a monotonic increase or decrease (model II), and a flat response (model I). The latter connotes that species abundance is unrelated to the environmental variable. Simplicity increases from model V to model I, because the number of estimated parameters declines (although models III and IV contain the same number of parameters). Oksanen and Minchin (2002) produced an algorithm for model selection that proceeds by fitting the most complex model (V) to the species data using maximum likelihood (with a Poisson error structure), and then by reducing model complexity (to IV, then to III, then to II, and finally to I) until deviance increases significantly (an F-ratio test fails, where $P \geq 0.05$). According to their routine, examination of model III occurs only after rejecting model IV over Model V. Therefore, model III may, in fact, represent a superior depiction of the response of some species allocated to model IV. We implemented this procedure for each species detected on at least ten plots and the three selected climate variables with HOF 2.3, an MS-DOS program (Oksanen and Minchin, 2002; available at http://cc.oulu.fi/~jarioksa/) for the quadrat and subplot frequency datasets. For both datasets, non-linear relationships to climate were statistically significant for most species, and the symmetrical unimodal function was the most common response type (Table 2).

We carried out CCA using the species data and three climate variables with PC-ORD 5.0 (McCune and Mefford, 2005). As Palmer (1993) found that CCA will not produce an artificial arch effect, a detrended version of CCA was unnecessary. We completed several CCA runs for each species dataset (quadrat frequencies and subplot frequencies). During a run, the program rescaled each plot score to a mean of zero and a variance of one, it calculated species scores as weighted means of plot scores, and it computed ordination axis scores as linear combinations of the constraining climate variables. For a given species dataset, we ran CCA for each climate variable individually to assess its statistical significance (the program executed a Monte Carlo test with 998 randomizations of the null hypothesis that no linear relationship exists between the matrix of species frequencies and a column matrix of climate values). We then performed an ordination with all significant climate variables to learn how they structured the species frequencies. To help evaluate the effectiveness of the latter, the program provided, for each ordination axis, a coefficient of determination (r^2) between Euclidean distance in the ordination space and relative Euclidean distance in the original species frequency space (McCune and

Table 2
Simplest statistically significant non-linear response models (HOF models) of relationship between climate variables and species with at least ten occurrences in the quadrat frequencies (Fq_i) and subplot frequencies (Fs_i) datasets. As explained in the text, the algorithm used to assign species to models may have overestimated the number of species characterized by model IV, and it may have underestimated the number of species with model III.

	MJAT	MJUT	MANPt
Quadrat frequencies			
Model V (skewed unimodal)	7	9	7
Model IV (symmetrical unimodal)	38	29	52
Model III (monotonic increase or decrease with plateau)	2	1	2
Model II (monotonic increase or decrease)	19	18	7
Model I (flat)	6	15	4
Total number of species = 72			
Subplot frequencies			
Model V (skewed unimodal)	8	6	5
Model IV (symmetrical unimodal)	61	46	77
Model III (monotonic increase or decrease with plateau)	3	1	1
Model II (monotonic increase or decrease)	23	28	18
Model I (flat)	12	26	6
Total number of species = 107			

MJAT = mean January temperature, MJUT = mean July temperature, MANPt = mean annual precipitation transformed to natural logarithms.

Grace (2002) recommend the use of relative Euclidean as a distance measure for the original space under CCA).

2.4. Calculation of transfer functions

We used weighted averaging-partial least squares regression (WA-PLS; Birks, 1998, and references therein) to estimate the transfer functions (β in Eq. (1)). A single WA-PLS run yields a transfer function for only one climate variable by constructing a model comprised of one or more components. WA-PLS, like CCA, assumes that species-climate response curves are unimodal and symmetrical. It produces an initial component as a set of coefficients, or weighted averages of the species optima (means, or distribution centers) with respect to a given climate variable. WA-PLS estimates the optima by inverse linear regression, i.e., it selects the optima so that their weighted averages best predict the values of the climate variable in the calibration set. Higher components use the residual structure in the data to improve the estimates of the optima. Identification of the model (number of components) that gives the best transfer function requires an examination of performance statistics generated by leave-one-out cross-validation (jackknifing). In general, a low RMSEP (root mean square error of prediction), a low maximum bias, no appreciable decline in r^2 (coefficient of determination), and a small number of components characterize the preferred model. WA-PLS has proved to be a robust method for building transfer functions. WA-PLS is well suited for analyzing datasets comprised of presence/absence or compositional species records with large numbers of species and many zero abundance values, considerable (but structured) noise, long compositional gradients (high beta diversity), and symmetrical unimodal response curves.

The characteristics of our data help justify the use of WA-PLS for transfer function construction: as argued previously, the frequency data used here reflect species abundances within plots. Nevertheless, they represent mathematical summaries of presence/absence data. The quadrat frequency database contains 538 species with 96% of the abundance values being zeros. The subplot frequency database includes 698 species with 95% zero abundance values. The plots included in the calibration set sample a broad array of geographical locations in a region known for its diversity in climate and other environmental characteristics (Franklin and Dyrness, 1988). Therefore, many variables, some behaving more-or-less randomly, others acting systematically, undoubtedly determine the species frequencies within a given plot. CCA will identify which of the climate variables structure the frequency data. During a WA-PLS run, all of these variables other than the one explicitly considered (and surely unidentified environmental variables as well) provide structured noise of potential use in improving model fit.

For each climate variable deemed important by CCA, we used C2 1.5.0 (Juggins, 2007) to perform two separate WA-PLS runs, one for each set of species data (quadrat frequencies and subplot frequencies). We generated performance statistics for each WA-PLS run through leave-one-out cross-validation.

Spatial autocorrelation within the calibration set (e.g., similar climate or species frequencies at nearby plots), if it affects the residuals (contained within δ of Eq. (1)), may lead to model overfitting (Telford and Birks, 2005, 2009; Telford, 2006). To check for spatial autocorrelation, we carried out a Mantel test (Mantel, 1967) for each of three datasets (quadrat frequencies, subplot frequencies, and plot-specific values for the selected climate variables) through PC-ORD 5.0 (McCune and Mefford, 2005). During a run, the program first converted the dataset to a Euclidean distance matrix. The program then performed a Monte Carlo test to evaluate its relationship to a matrix of inter-plot horizontal distances in meters (we ignored elevational variations between plots) by permuting (1000 times) the rows and columns of one of the matrices. Rejection of the null hypothesis of no relationship between the two matrices provides evidence that the dataset contains spatially autocorrelated information.

3. Results

3.1. Importance of climate variables

The results of CCA demonstrate that MJAT, MJUT, and MANPt substantially influence the frequencies of vascular plants (both quadrat frequencies and subplot frequencies) in the calibration dataset. The outcomes for quadrat and subplot frequencies were nearly identical. For brevity, we present the results only for the former.

We found no evidence of multivariate outliers during any of the runs, so we used the full dataset (538 species and 107 plots).

CCA performed separately for the three relatively non-multicollinear climate variables indicated that MJAT, MJUT, and MANPt explain 2.9%, 2.4%, and 3.2% of the variance among species in the space defined by a single climate variable (ratio of the eigenvalue for the first and only canonical axis to the total explainable variance), respectively. We are not surprised by such small percentages given the large number of species, numerous zero abundance values, and noise contained in the quadrat frequencies database. Nevertheless, all three climate variables exert statistically significant influences on species frequency: For each CCA run, a Monte Carlo test showed that the proportion of randomized runs with an eigenvalue greater than or equal to the eigenvalue actually associated with the first axis (P) is 0.001.

Table 3 summarizes the results of CCA as constrained by all three (statistically significant) climate variables for quadrat frequencies. The first of three canonical axes captured most of the variation in the ordination, with a coefficient of determination (r^2) of 0.22. Axis 1 is a precipitation gradient, with an almost perfect positive intraset correlation with MANPt. MJAT displays a moderately high (and positive) correlation with the same axis, possibly revealing a gradient of "continentality". However, inspection of ordination scores revealed that species near one end of axis 1 tolerate scarce precipitation, but not necessarily cold

Table 3
Canonical correspondence analysis (CCA) for quadrat frequencies (Fq_i) of 538 vascular plant species on 107 plots as constrained by three statistically significant climate variables: summary statistics.

	Axis 1	Axis 2	Axis 3
Coefficient of determination (r^2)	0.22	0.06	−0.07
Intraset correlations (here, same as biplot scores)			
MJAT	0.67	0.74	0.08
MJUT	−0.23	0.87	−0.45
MANPt	0.98	−0.20	−0.05
Interset correlations			
MJAT	0.65	0.70	0.07
MJUT	−0.22	0.83	−0.39
MANPt	0.94	−0.19	−0.05
Inertia = 23.48			
Eigenvalue	0.76	0.61	0.33

MJAT = mean January temperature, MJUT = mean July temperature, MANPt = mean annual precipitation transformed to natural logarithms.

Table 4
Weighted averaging-partial least squares regression (WA-PLS) of quadrat frequencies (Fq_i) for each of three climate variables: performance statistics generated by leave-one-out cross-validation (jackknifing).

Climate variable	Component	RMSEP	Maximum bias	r^2
MJAT	1	1.79 °C	3.61 °C	0.81
	2[a]	1.62 °C	2.94 °C	0.85
	3	1.66 °C	2.98 °C	0.84
	4	1.69 °C	2.99 °C	0.83
	5	1.70 °C	3.06 °C	0.83
MJUT	1	1.47 °C	6.54 °C	0.58
	2[a]	1.39 °C	6.08 °C	0.64
	3	1.40 °C	6.28 °C	0.62
	4	1.42 °C	6.20 °C	0.61
	5	1.42 °C	6.14 °C	0.61
MANPt	1	0.28	0.73	0.83
	2[a]	0.27	0.66	0.85
	3	0.27	0.71	0.85
	4	0.27	0.70	0.84
	5	0.27	0.68	0.84

RMSEP = root mean square error of prediction, r^2 = coefficient of determination, MJAT = mean January temperature, MJUT = mean July temperature, MANPt = mean annual precipitation transformed to natural logarithms.
[a] Preferred model.

winters (continental climates have low MANPt and low MJAT). Species near the other extreme of axis 1 enjoy copious precipitation, but not necessarily warm winters (maritime climates have high MANPt and high MJAT).

Axis 2 is a relatively weak climate gradient, with an r^2 of 0.06. Both MJAT and MJUT are highly (and positively) linked to axis 2, indicating that it is a temperature gradient.

The small and negative r^2 of axis 3 (−0.07) may reflect the optimization of some criterion unrelated to the percentage of variance extracted (McCune and Grace, 2002). The magnitudes of all intraset correlations with axis 3 are small to modest, indicating that the third axis is of no use in assessing the roles of the selected climate variables in structuring the quadrat frequencies data.

The CCA ordination biplot graph (Fig. 2) provides visual details about the climatic correlates of the two useful ordination axes. Each climate variable arrow is based on the interset correlations and eigenvalues; the length and angle indicates the strength of the correlation between the variable and axis. *Luzula arcuata*, a graminoid appearing on the right side of the ordination and close to axis 1, occurred on a single plot in the wet, maritime-influenced western hemlock (*Tsuga heterophylla*) forest of the Coast Range in Washington. *Antennaria rosea*, which appears on the left side of the ordination and close to axis 1, inhabits the dry Ponderosa pine (*Pinus ponderosa*) and Douglas-fir (*Pseudotsuga menziesii*) forests of northeastern and southeastern Washington. At the bottom of the figure and close to axis 2, is a set of seven species (*Antennaria lanata*, *Erigeron aureus*, *Erigeron lonchophyllus*, *Festuca viridula*, *Potentilla drummondii*, *Ranunculus verecundus*, and *Veronica serpyllifolia*) found on a plot in the high-elevation lodgepole pine (*Pinus contorta*) forest in the North Cascades of Washington where temperatures are relatively low. *Rupertia physodes*, which appears near the top of the figure and close to axis 2, occurs on only one plot in the warm Douglas-fir forest of the Klamath Mountains in southwestern Oregon.

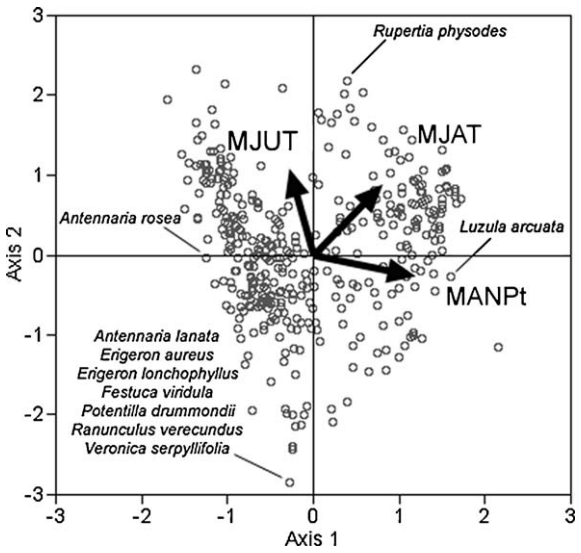

Fig. 2. Canonical correspondence analysis (CCA) for quadrat frequencies (Fq_i) of 538 vascular plant species on 107 plots as constrained by three statistically significant climate variables: ordination biplot graph of the first two canonical axes. Each point approximates the weighted average of a species with respect to the climate variables represented by the axes. In some cases, several species share the same point. The biplot scores of Table 3 provide the coordinates for the head of each climate variable arrow. We discuss the four labeled points in the text.

3.2. Transfer functions

The abilities of WA-PLS to predict the three climate variables shown to be important by CCA (MJAT, MJUT, and MANPt), as assessed by leave-one-out cross-validation, were quite similar for both species databases (quadrat frequencies and subplot frequencies). Therefore, we present the complete results only for the WA-PLS runs based on quadrat frequencies.

We removed no species or plots as supposed outliers from the quadrat frequencies dataset (538 species and 107 plots). Table 4 gives performance statistics. For all three WA-PLS runs (one for each of three climate variables), we identified two-component models as the most desirable. In all three cases, the two-component model yielded the minimal RMSEP (root mean square error of prediction), the minimal maximum bias, and the maximal r^2 (coefficient of determination). Fig. 3 permits a graphical evaluation of the performance of the two-component WA-PLS model for each climate variable. The scatter plots clearly reveal pronounced systematic bias in the predictions for all three of the climate variables (the models overestimate the climate values near the lower ends of the ranges and underestimate them near the upper ends of the ranges) a common shortcoming of WA-PLS (Ter Braak and Juggins, 1993; Birks, 1998).

Only minor differences in performance, as indicated in Table 5, distinguished the results of WA-PLS (two-component models) for

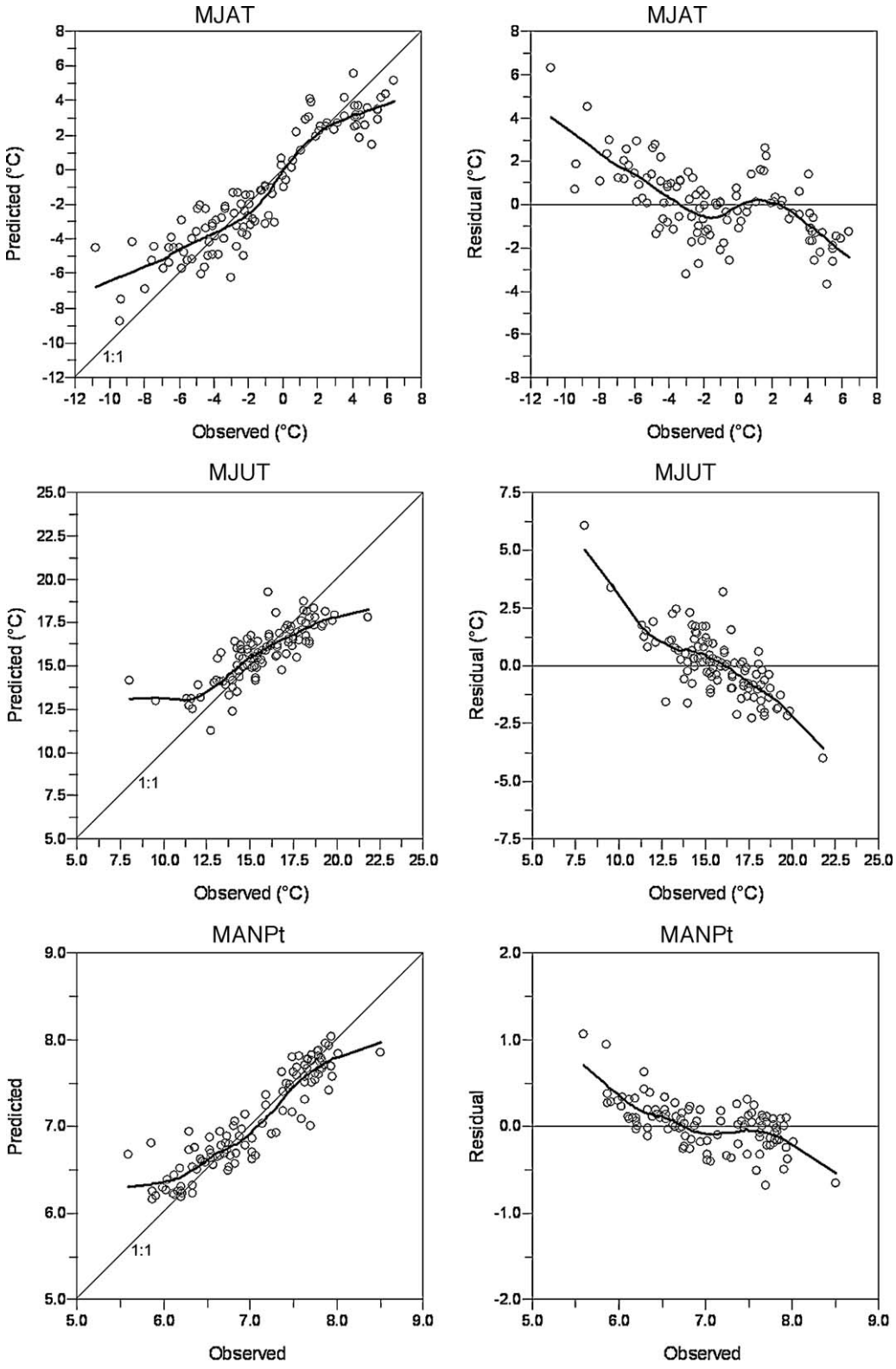

Fig. 3. Weighted averaging-partial least squares regression (WA-PLS) of quadrat frequencies (Fq_i): scatter plots of predicted (by leave-one-out cross-validation [jackknifing]) vs. observed value and residual (predicted-observed) vs. observed value based on the two-component model for MJAT, MJUT, and MANPt. The heavy lines are LOESS (locally weighted polynomial regression; span = 0.45) fits intended to accentuate patterns within the scatter plots.

the quadrat frequencies and subplot frequencies datasets. For MJAT, RMSEP (root mean square error of prediction) was about 12% lower for subplot frequencies. The maximum biases associated with subplot frequencies were approximately 17% lower for MJUT, but around 10% higher for MANPt.

The Mantel tests revealed that, indeed, the calibration set shows significant spatial autocorrelation. The Monte Carlo tests yielded *P* values of 0.012, 0.001, and 0.001, respectively, for quadrat frequencies, subplot frequencies, and climate data (MJAT, MJUT, and MANPt). For each dataset, we were compelled to reject the null

Table 5
Weighted averaging-partial least squares regression (WA-PLS) for each of three climate variables: comparison of performance statistics associated with the (preferred) two-component models for quadrat frequencies (Fq_i) subplot frequencies (Fs_i).

Climate variable	Species dataset	RMSEP	Maximum bias	r^2
MJAT	Fq_i	1.62 °C	2.94 °C	0.85
	Fs_i	1.43 °C	2.67 °C	0.89
MJUT	Fq_i	1.39 °C	6.08 °C	0.64
	Fs_i	1.39 °C	5.05 °C	0.63
MANPt	Fq_i	0.27	0.66	0.85
	Fs_i	0.26	0.77	0.86

RMSEP = root mean square error of prediction, r^2 = coefficient of determination, MJAT = mean January temperature, MJUT = mean July temperature, MANPt = mean annual precipitation transformed to natural logarithms.

hypothesis of no correlation with inter-plot geographical distances. Plots that are close to each other tend to have similar species frequencies and climatic conditions.

4. Discussion

We created a calibration set consisting of contemporary vascular plant species abundances (both quadrat and subplot frequencies) and climate data for 107 FIA plots in Oregon and Washington. Through WA-PLS, we created six transfer functions to enable the prediction of MJAT (mean January temperature), MJUT (mean July temperature), and MANPt (mean annual precipitation transformed to natural logarithms) from quadrat or subplot frequencies measured, in the future, on those plots. We assessed the predictive abilities of the transfer functions (all are two-component WA-PLS models) by leave-one-out cross-validation.

We expected the transfer functions based on subplot frequencies to prove superior, because the subplot frequencies database contains more species (698) than the quadrat frequencies database (538). However, the choice of species database had little effect on performance.

The coefficients of determination (r^2) linked to the transfer functions for MJAT and MANPt are very high (0.85 or greater). Recent palaeoecological studies with comparable statistical methods (Lu et al., 2006; Shen et al., 2006; Finsinger et al., 2007) found similar values for mean January temperature and (untransformed) mean annual precipitation transfer functions. Our MJUT transfer functions are much less powerful (r^2 = 0.63–0.64). A large range of r^2 statistics (0.33–0.84) characterized mean July temperature transfer functions in recent palaeoecological investigations with analogous methods (Rosén et al., 2003; Shen et al., 2006; Finsinger et al., 2007). RMSEPs expressed as percentages of variable ranges, are similar to, or slightly better than, recently published values for our temperature transfer functions (8.31–10.12%). Absolute errors (back-transformed RMSEPs that depend on the position along the gradient) expressed as percentages of the range of mean annual precipitation lie between about 2% and 33% for our MANPt transfer functions. The corresponding relative errors (back-transformed RMSEPs that are independent of gradient position) are close to 30%. Due to transformation, the RMSEPs associated with our MANPt transfer functions are not readily comparable to published values for mean annual precipitation, although our RMSEPs for the dry end of the precipitation gradient are appreciably lower than recently published percentages for untransformed mean annual precipitation transfer functions (7.25–8.00%; Lu et al., 2006; Shen et al., 2006). We had expected our transfer functions to significantly outperform the paleoecological ones, as our frequency data represent direct measures of plot-specific species abundances, i.e., they are unaffected by pollen grain/spore/phytolith production rates, transport to sedimentary basins, and taphonomic processes.

The scatter plots (Fig. 3) show that the transfer functions successfully predict the overall trends inherent in the observed climate values within the calibration set. However, the relationship between observed and predicted values is not perfect: many residuals deviate substantially from zero. Such deviance is due to systematic bias (expressed by maximum bias) and random variability (embodied in RMSEP). The former includes the tendency of WA-PLS to produce overestimates near the lower ends of the climate ranges and underestimates near the opposite ends. The latter results from plot-specific non-climatic factors (natural disturbance and secondary succession, soil characteristics, anthropogenic forces, and historical peculiarities) that influence species frequencies.

The discovery of statistically significant spatial autocorrelation within the calibration set constitutes a warning that the transfer function performance statistics generated from the calibration set itself by leave-one-out cross-validation may have been over-optimistic (Telford and Birks, 2005, 2009; Telford, 2006). To avoid this problem, we would have had to base the calculation of performance statistics on a spatially independent test set, not on the calibration set. While construction of such a test set would not have been feasible, WA-PLS models are fairly robust to spatial autocorrelation.

4.1. Accounting for transfer function performance

Both data quality and statistical considerations likely are responsible for the good predictive abilities of our transfer functions.

We computed the vascular plant species frequencies from inventory data for FIA Phase 3 plots. An elaborate quality assurance program helps to maintain the veracity of plot data. This includes the training, testing, and certification of experienced botanists as well as field audits (Pollard, nd; Schulz, nd). Gray and Azuma (2005) reported the outcome of an assessment of data collector precision involving two botanists (working independently) and 48 FIA Phase 3 plots from Oregon sampled in 2000: The botanists agreed on species identifications 71% of the time (Sørensen's index of similarity) within subplots and 67% of the time within quadrats. The researchers concluded that differences of opinion generally concerned congeneric species or the missing of rare plants, and that repeatability was comparable to results of other botanical studies. The species data we used here sampled 20–30% of the plot locations potentially examined for these states over a full measurement cycle. A larger species dataset possibly would contain fewer zeros and reveal stronger relationships with estimated climate.

For each plot, we obtained climate data from the Daymet model database. Thornton et al. (1997) carried out a leave-one-out cross-validation analysis to evaluate the predictive ability of Daymet. They compared modeled daily maximum temperature, daily minimum temperature, and daily precipitation with actual measurements over 1 year (1989) at nearly 500 sites in the inland northwestern USA (including southeastern Washington and northeastern Oregon). Mean absolute error of prediction, MAE, and bias were 0.7 and −0.1 °C, respectively, for the annual mean of daily maximum temperature. MAE and bias were 1.2 and 0.1 °C, respectively, for the annual mean of daily minimum temperature. MAE and bias were 134 and −21 mm, respectively, for annual precipitation. These variables and performance statistics differ from those used in our study. However, according to the authors, the prediction errors associated with the temperature variables are comparable to published values for other climate models. Daymet

successfully predicted the occurrence of daily precipitation 83.3% of the time, a seemingly commendable rate.

The transformation of mean annual precipitation to natural logarithms is responsible, probably primarily, for the good performances of our transfer functions for MANPt (very high r^2 values; very low RMSEPs at the dry end of the gradient). We obtained transfer functions with remarkably poor performance statistics after applying WA-PLS to untransformed mean annual precipitation data (MANP). The unsatisfactory outcomes included the one-component models, which suggest that the advantages of transformation emerge when determining weighted averages for the original environmental variable. Prior to transformation, MANP was badly skewed, so we expected many species response curves to exhibit considerable skewness as well. In fact, when we fitted HOF models to quadrat frequencies data and MANP (we used the same methods as described above), the symmetrical unimodal curve (Model IV) still was the dominant type, but the number of species responses characterized by it declined substantially. In contrast, the monotonic increasing or decreasing curve (Model II) became much more common. When response curves are not symmetrical, weighted averaging will provide poor estimates of species optima, which leads to a defective WA-PLS transfer function. Transformation of MANP reduced the distortion by reducing or eliminating the skewness in many species response curves. The logic here is somewhat akin to that used to explain the effects of sampling evenness on weighted average estimates of species optima (Ter Braak and Looman, 1986). Logarithmic or square-root transformation of environmental data is no guarantee of good results. Such transformations of our temperature data failed to yield improved transfer functions (the transformation of temperature data makes little ecological sense anyway). Clearly, simulation studies are warranted to identify the consequences of environmental data transformation on transfer function construction by WA-PLS.

4.2. Capability of detecting future climate change

The primary objective of this research is to develop a set of transfer functions that can provide high quality quantitative information about future local climatic conditions based on future measurements of vascular plant species frequencies on FIA Phase 3 plots. The usefulness of our transfer functions rests upon their abilities to detect short-term changes in climate. The magnitude of its predictive error (i.e., RMSEP and maximum bias) and the pace of climate change expected over the coming decades establish the apparent resolution of each transfer function. The actual predictive power of a transfer function also hinges on the rates of response of species frequencies to climate change (i.e., the relative lengths of lags).

As reported by Mote et al. (2008), the Climate Impacts Group at the University of Washington evaluated 20 global simulation models to develop predictions of future climate (30-year means for selected variables) in the Pacific Northwest, USA, which includes Oregon and Washington. Each of the models had produced simulations for scenarios of low (scenario B1) and high (scenario A1B) projected changes in future concentrations of greenhouse gases, which promote atmospheric warming, and sulfate aerosols, which partly ameliorate warming. For a given emissions scenario and climate variable, the Climate Impacts Group determined the amount of change, specific to the Pacific Northwest, predicted by each of the 20 models relative to an average for 1970–1999. They also computed a weighted average of the 20 predictions (models that performed well in simulating twentieth century climate received greater weight).

Fig. 4 facilitates the assessment of the apparent abilities of our transfer functions to detect the climate changes expected for

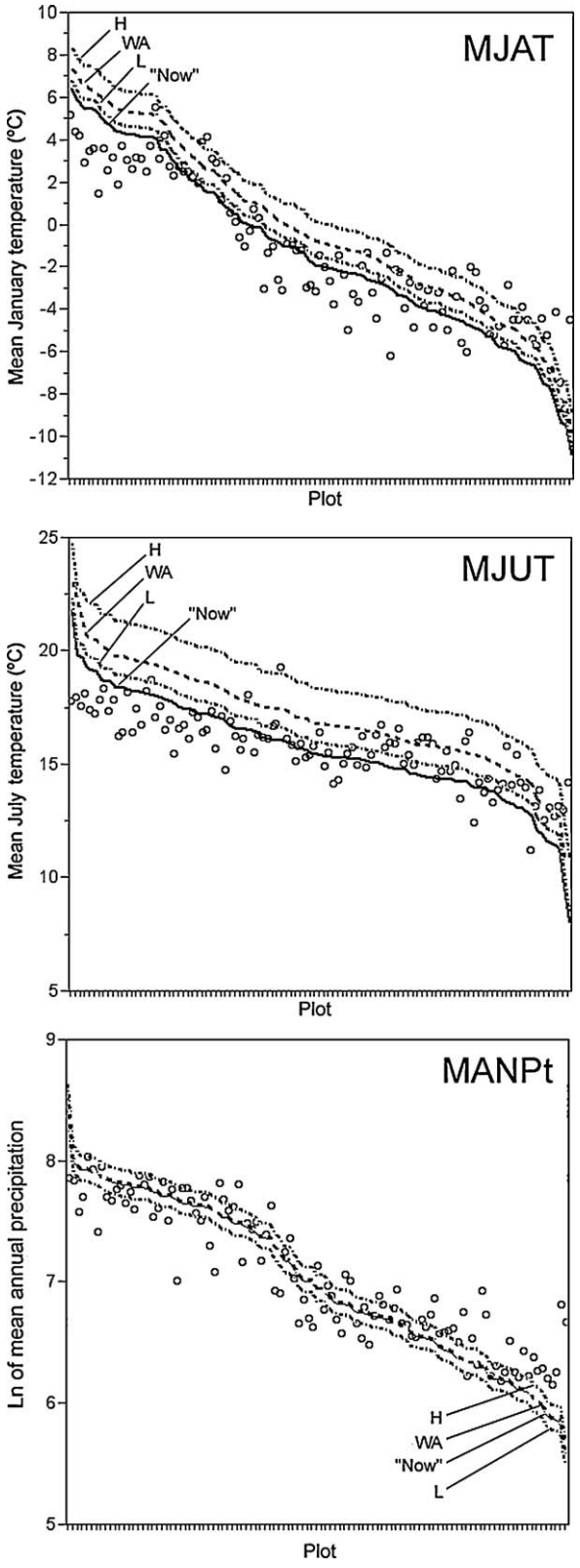

Fig. 4. Assessing the potentials of our MJAT, MJUT, and MANPt transfer functions to ascertain the climate changes predicted for Oregon and Washington by global models for the first 30-year period of this century. "Now" lines show observed climate for 107 Oregon and Washington plots from calibration set (in order from high to low). Points denote climate predicted by two-component WA-PLS model for quadrat frequencies, Fq_i, for same plots. H lines depict climate given the highest model prediction for 2000–2029. WA lines depict climate given the weighted average model prediction for 2000–2029. L lines depict climate given the lowest model prediction for 2000–2029.

Oregon and Washington by global models for the period 2010–2039. Each graph shows the observed and predicted (by two-component WA-PLS model for quadrat frequencies) climate values for plots from the calibration set (1980–1997) as well as the lowest, highest, and weighted average model predictions for 2010–2039. We obtained the data generated by the Climate Impacts Group at http://cses.washington.edu/cig/fpt/08scensumdata.shtml. This source does not offer temperature predictions by month. Therefore, we based predicted changes in MJAT on those for mean winter (December, January, February) temperature, and predicted changes in MJUT on those for mean summer (June, July, August) temperature. Since scenarios B1 and A1B give similar results prior to the 2050s, we averaged the weighted averages calculated under these opposing propositions. To obtain future climate values, we simply added the predicted changes to the estimated Daymet values for all plots from the calibration set (1980–1997). Note that we assumed that all plots experience the same amount of change over a given interval of time. This seems reasonable, as twentieth century patterns of change in temperature and precipitation were roughly uniform across the Pacific Northwest (Mote, 2003).

Our transfer functions will possess sufficient resolution for detecting the climatic trends expected to characterize Oregon and Washington during the first part of this century only if the amount of change taking place significantly exceeds the sizes of the predictive errors estimated by leave-one- out cross-validation, and if the lags of at least a fair number of species are no more than several decades in length. As is evident from Fig. 4, the errors associated with the MJAT transfer functions are great enough that even the highest amount of change predicted for the period 2010–2039 would be indistinguishable from current climatic conditions. On the other hand, the MJUT transfer functions have the abilities to detect change under the highest projection for 2010–2039. The results of 20 global models indicate that only slight changes in mean annual precipitation will occur during the early part of the twenty-first century. If the predictions are correct, our MANPt transfer functions will have no new climatic trend to monitor.

Our MJUT transfer functions may become useful soon in view of the rapid rate of increase in summer temperatures expected during the first few decades of this century by some global simulation models. The higher model predictions indicate that our MJAT transfer functions may be able to track changes in mean January temperature by the 2040s. In addition, the higher model predictions suggest that our MANPt transfer functions may begin detecting changes in mean annual precipitation by the 2070s. Of course, our MJAT and MANPt transfer functions may prove useful at the present time to verify relative climatic stability (assuming that lags are very short).

Fig. 4 attests to the general correlation between observed climate values and those predicted by our transfer functions. Because the predicted values sometimes deviate substantially from the observed values for individual plots, our transfer functions are appropriate for monitoring climatic trends over the entire Pacific Northwest or large regions within it, not for assessing climate change at individual plots.

5. Conclusions

To monitor future climate changes in Oregon and Washington, we exploited the link between vascular plant species abundance and climate: We assembled a calibration set consisting of present-day quadrat and subplot species frequencies and climate estimates for 107 FIA Phase 3 plots. We used WA-PLS to calculate six transfer functions that will permit the prediction of MJAT (mean January temperature), MJUT (mean July temperature), and MANPt (mean annual precipitation transformed to natural logarithms) from future quadrat or subplot frequency measurements.

Our transfer functions possess good predictive abilities compared to those reported in the literature. Both data quality and statistical considerations (viz., the logarithmic transformation of mean annual precipitation) probably are responsible. The discovery of spatial autocorrelation in the calibration set may portend some inflation of the apparent predictive abilities of our transfer functions.

Our MJUT transfer functions may become useful soon in view of the rapid rate of increase in summer temperatures expected during the first few decades of this century by some global simulation models. Our MJAT transfer functions may be able to track changes in mean January temperature by the 2040s. Our MANPt transfer functions may begin detecting changes in mean annual precipitation by the 2070s. Our MJAT and MANPt transfer functions can be used soon to verify relative climatic stability, if lags are very short.

Our transfer functions, whether based on quadrat frequencies or on subplot frequencies, successfully predict the overall climatic trends in the calibration set. However, because the predicted and observed values sometimes deviate substantially for individual plots, our transfer functions are appropriate for monitoring regional climatic patterns, not for assessing climate change at specific plots.

Acknowledgements

J. Morefield, J. Pijoan, C. Grenz, and S. Butler collected field data. S. Sundberg and K. Mitchell (Oregon State University Herbarium) identified voucher specimens. R. S. Creagan edited the References section. J. S. Fried and two anonymous reviewers commented on earlier versions of the manuscript.

References

Andrewartha, H.G., Birch, L.C., 1954. The Distribution and Abundance of Animals. University of Chicago Press, Chicago.
Belsley, D.A., Kuh, E., Welsch, R.E., 1980. Regression Diagnostics: Identifying Influential Data and Sources of Collinearity. Wiley, New York.
Birks, H.J.B., 1995. Quantitative palaeoenvironmental reconstructions. In: Maddy, D., Brew, J.S. (Eds.), Statistical Modelling of Quaternary Science Data, Technical Guide, vol. 5. Quaternary Research Association, Cambridge, pp. 161–254.
Birks, H.J.B., 1998. Numerical tools in palaeolimnology-progress, potentialities, and problems. J. Palaeolimnol. 20, 307–332.
Cleland, D.T., Freeouf, J.A., Keys Jr., J.E., Nowacki, G.J., Carpenter, C.A., McNab, W.H., 2007. Ecological Subregions: Sections and Subsections for the Conterminous United States [1:3,500,000] [CD-ROM]. USDA Forest Service, Washington, D.C..
Davis, M.B., Botkin, D.B., 1985. Sensitivity of the fossil pollen record to sudden climatic change. Quat. Res. 23, 327–340.
Enright, J.T., 1976. Climate and population regulation: the biogeographers dilemma. Oecologia 24, 295–310.
Finsinger, W., Heiri, O., Valsecchi, V., Tinner, W., Lotter, A.F., 2007. Modern pollen assemblages as climate indicators in southern Europe. Global Ecol. Biogeogr. 16, 567–582.
Franklin, J.F., Dyrness, C.T., 1988. Natural Vegetation of Oregon and Washington. Oregon State University Press, Corvallis.
Garbolino, E., De Ruffray, P., Brisse, H., Grandjouan, G., 2007. Relations entre plantes et climats en France: étalonnage de 1874 bio-indicateurs. C. R. Biologies 330, 159–170.
Gray, A.N., Azuma, D.L., 2005. Repeatability and implementation of a forest vegetation indicator. Ecol. Indicators 5, 57–71.
Hartmann, H.C., Pagano, T.C., Sorooshian, S., Bales, R., 2002. Confidence builders: evaluating seasonal climate forecasts from user perspectives. Bull. Am. Meteorol. Soc. 83, 683–698.
Hill, M.O., Gauch Jr., H.G., 1980. Detrended correspondence analysis: an improved ordination technique. Vegetatio 42, 47–58.
Howe, S., Webb III, T., 1983. Calibrating pollen data in climatic terms: improving the methods. Quat. Sci. Rev. 2, 17–51.
Huisman, J., Olff, H., Fresco, L.F.M., 1993. A hierarchical set of models for species response analysis. J. Veg. Sci. 4, 37–46.
IPCC, 2007. Summary for policymakers. In: Solomon, S., Qin, D., Manning, M., Chen, Z., Marquis, M., Averyt, K.B., Tignor, M., Miller, H.L. (Eds.), Climate Change 2007: The Physical Science Basis. Contribution of Working Group I to the Fourth Assessment Report of the Intergovernmental Panel on Climate Change. Cambridge University Press, Cambridge.
Juggins, S., 2007. C2 (version 1.5.0), a Microsoft Windows Program for the Analysis and Visualization of Ecological and Palaeoenvironmental Data. Available at http://www.campus.ncl.ac.uk/staff/Stephen.Juggins.

Karlsen, S.R., Elvebakk, A., 2003. A method using indicator plants to map local climatic variation in the Kangerlussuaq/Scoresby Sund area, East Greenland. J. Biogeogr. 30, 1469–1491.
Krebs, C.J., 1985. Ecology: The Experimental Analysis of Distribution and Abundance, 3rd ed. Harper and Row, New York.
Leps, J., Smilauer, P., 2003. Multivariate Analysis of Ecological Data Using CANOCO. Cambridge University Press, Cambridge, UK.
Li, Y., Xu, Q., Liu, J., Yang, X., Nakagawa, T., 2007. A transfer-function model developed from an extensive surface-pollen data set in northern China and its potential for palaeoclimate reconstructions. Holocene 17, 897–905.
Lischke, H., Lotter, A.F., Fischlin, A., 2002. Untangling a Holocene pollen record with forest model simulations and independent climate data. Ecol. Model. 150, 1–21.
Lu, H., Wu, N., Yang, X., Jiang, H., Liu, K., Liu, T., 2006. Phytoliths as quantitative indicators for the reconstruction of past environmental conditions in China I: phytolith-based transfer functions. Quat. Sci. Rev. 25, 945–959.
Mantel, N., 1967. The detection of disease clustering and generalized regression approach. Cancer Res. 27, 209–220.
Marquardt, D.W., 1970. Generalized inverses, ridge regression, biased linear estimation, and nonlinear estimation. Technometrics 12 (591), 605–607.
McCune, B., Grace, J.B., 2002. Analysis of Ecological Communities. MjM Software, Gleneden Beach, Oregon, USA.
McCune, B., Mefford, M.J., 2005. PC-ORD (version 5.0), a Microsoft Windows Program for the Multivariate Analysis of Ecological Data. MjM Software, Gleneden Beach, Oregon, USA.
Miles, E.L., Snover, A.K., Whitely Binder, L.C., Sarachik, E.S., Mote, P.W., Mantua, N., 2006. An approach to designing a national climate service. Proc. Natl. Acad. Sci. 103, 19616–19623.
Miller, P.A., Giesecke, T., Hickler, T., Bradshaw, R.H.W., Smith, B., Seppä, H., Valdes, P.J., Sykes, M.T., 2008. Exploring climatic and biotic controls on Holocene vegetation change in Fennoscandia. J. Ecol. 96, 247–259.
Mote, P.W., 2003. Trends in temperature and precipitation in the Pacific Northwest during the twentieth century. Northwest Sci. 77, 271–282.
Mote, P.W., Salathé, E.P., Dulière, V., Jump, E., 2008. Scenarios of Future Climate Change for the Pacific Northwest. Report prepared by the Climate Impacts Group, Center for Science in the Earth System, Joint Institute for the Study of the Atmosphere and Oceans, University of Washington, Seattle. Available at http://cses.washington.edu/db/pubs/abstract578.shtml.
Neumann, F., Schoelzel, C., Litt, T., Hense, A., Stein, M., 2007. Holocene vegetation and climate history of the northern Golan heights (Near East). Veg. Hist. Archaeobot. 16, 329–346.
Økland, R.H., 1986. Reseating of ecological gradients. II. The effect of scale on symmetry of species response curves. Nordic J. Bot. 6, 661–670.
Oksanen, J., Minchin, P.R., 2002. Continuum theory revisited: what shape are species responses along ecological gradients? Ecol. Model. 157, 119–129.
Palmer, M.W., 1993. Putting things in even better order: the advantages of canonical correspondence analysis. Ecology 74, 2215–2230.
Payette, S., 2007. Contrasted dynamics of Northern Labrador tree lines caused by climate change and migrational lag. Ecology 88, 770–780.
Pollard, J., nd. Forest Inventory and Analysis: Quality Assurance. FIA Fact Sheet Series. Available at http://fia.fs.fed.us/library/fact-sheets/.
Prentice, I.C., Monserud, R.A., Smith, T.M., Emanuel, W.R., 1993. Modeling large-scale vegetation dynamics. In: Solomon, A.M., Shugart, H.H. (Eds.), Vegetation Dynamics and Global Change. Chapman and Hall, New York, pp. 235–250.
Rosén, P., Segerstrom, U., Eriksson, L., Renberg, I., 2003. Do diatom, chironomid, and pollen records consistently infer Holocene July air temperature? A comparison using sediment cores from four alpine lakes in northern Sweden. Arctic Antarctic Alpine Res. 35, 279–290.
Sachs, H.M., Webb III, T., Clark, D.R., 1977. Paleoecological transfer functions. Ann. Rev. Earth Planet. Sci. 5, 159–178.
SAS Institute Inc., 2000. JMP (version 4.0.2). Cary, NC, 1989–2007.
Schulz, B.K., nd. Forest Inventory and Analysis: Vegetation Indicator. FIA Fact Sheet Series. Available at http://fia.fs.fed.us/library/fact-sheets/.
Schulz, B.K., Bechtold, W.A., Zarnoch, S.J., 2009. Sampling and Estimation Procedures for the Vegetation Diversity and Structure Indicator. PNW-GTR-781. USDA Forest Service, Pacific Northwest Research Station, Portland, OR.
Shen, C., Liu, K., Tang, L., Overpeck, J.T., 2006. Quantitative relationships between modern pollen rain and climate in the Tibetan Plateau. Rev. Palaeobot. Palynol. 140, 61–77.
Smith, A.G., 1965. Problems of inertia and threshold related to postglacial habitat changes. Proc. R. Soc. Lond., Ser. B 61, 331–342.
Smith, S.D., Bunting, S.C., Hironaka, M., 1986. Sensitivity of frequency plots for detecting vegetation change. Northwest Sci. 60, 279–286.
Stapanian, M.A., Cline, S.P., Cassell, D.L., 1997. Evaluation of a measurement method for forest vegetation in a large-scale ecological survey. Environ. Monit. Assess. 45, 237–257.
St. Jacques, J., Cumming, B.F., Smol, J.P., 2008. A pre-European settlement pollen–climate calibration set for Minnesota, USA: developing tools for palaeoclimatic reconstructions. J. Biogeogr. 35, 306–324.
Svenning, J.-C., Normand, S., Skov, F., 2008. Postglacial dispersal limitation of widespread forest plant species in nemoral Europe. Ecography 31, 316–326.
Telford, R.J., 2006. Limitations of dinoflagellate cyst transfer functions. Quat. Sci. Rev. 25, 1375–1382.
Telford, R.J., Birks, H.J.B., 2005. The secret assumption of transfer functions: problems with spatial autocorrelation in evaluating model performance. Quat. Sci. Rev. 24, 2173–2179.
Telford, R.J., Birks, H.J.B., 2009. Evaluation of transfer functions in spatially structured environments. Quat. Sci. Rev. 28, 1309–1316.
Ter Braak, C.J.F., 1986. Canonical correspondence analysis: a new eigenvector technique for multivariate direct gradient analysis. Ecology 67, 1167–1179.
Ter Braak, C.J.F., 1987. The analysis of vegetation-environment relationships by canonical correspondence analysis. Vegetatio 69, 69–77.
Ter Braak, C.J.F., 1995. Non-linear methods for multivariate statistical calibration and their use in palaeoecology: a comparison of inverse (k-nearest neighbours), partial least squares and weighted averaging partial least squares and classical approaches. Chemomet. Intell. Lab. Syst. 28, 165–180.
Ter Braak, C.J.F., Juggins, S., 1993. Weighted averaging partial least squares regression (WA-PLS): an improved method for reconstructing environmental variables from species assemblages. Hydrobiologia 269/270, 485–502.
Ter Braak, C.J.F., Looman, C.W.N., 1986. Weighted averaging, logistic regression and the Gaussian response model. Vegetatio 65, 3–11.
Ter Braak, C.J.F., Prentice, I.C., 1988. A theory of gradient analysis. Adv. Ecol. Res. 18, 271–317.
Thornton, P.E., Running, S.W., White, M.A., 1997. Generating surfaces of daily meteorological variables over large regions of complex terrain. J. Hydrol. 190, 214–251.
Valsecchi, V., Finsinger, W., Tinner, W., Ammann, B., 2008. Testing the influence of climate, human impact and fire on the Holocene population expansion of *Fagus sylvatica* in the southern Prealps (Italy). Holocene 18, 603–614.
Webb III, T., 1986. Is vegetation in equilibrium with climate? How to interpret late-Quaternary pollen data. Vegetatio 67, 75–91.
Wilmshurst, J.M., McGlone, M.S., Leathwick, J.R., Newnham, R.M., 2007. A pre-deforestation pollen-climate calibration model for New Zealand and quantitative temperature reconstructions for the past 18,000 years BP. J. Quat. Sci. 22, 535–547.
Woodward, F.I., 1987. Climate and Plant Distribution. Cambridge University Press, Cambridge.
Woodward, F.I., 1992. Predicting plant responses to global environmental change. New Phytol. 122, 239–251.
Woodward, F.I., Williams, B.G., 1987. Climate and plant distribution at global and local scales. Vegetatio 69, 189–197.